Available online at www.sciencedirect.com
ScienceDirect
International Journal of Heat and Mass Transfer 51 (2008) 4195–4203
International Journal of HEAT and MASS TRANSFER
www.elsevier.com/locate/ijhmt

Effects of turbulence and inlet moisture on two-phase spontaneously condensing flows in transonic nozzles

A.R. Avetissian [a,*], G.A. Philippov [a], L.I. Zaichik [b]

[a] All Russian Nuclear Power Engineering Research and Development Institute, Cosmonaut Volkov Street 6a, 125171 Moscow, Russia
[b] Nuclear Safety Institute of the Russian Academy of Sciences, B. Tulskaya 52, 115191 Moscow, Russia

Received 10 September 2007; received in revised form 11 October 2007
Available online 9 May 2008

Abstract

The objective of the paper is to analyse the effects of flow turbulence and inlet moisture on the process of spontaneous condensation of supercooled steam. Calculations of steady and unsteady spontaneously condensing transonic turbulent flows in Laval nozzles are presented. Comparisons of model predictions with experimental data are discussed.

Keywords: Two-phase transonic flow; Droplets; Nucleation; Condensation; Turbulence

1. Introduction

Two-phase droplet-laden flows are frequently encountered in environmental contexts and industrial applications, such as the formation of contrails from aircraft exhausts, the combustion of liquid sprays, and the condensation of steam in turbines. Traditionally, two-phase transonic flows in Laval nozzles and turbine blade cascades are modeled in an approximation that ignores the effects of viscosity, thermal conductivity, and turbulence (e.g. [1–6]). The disregard of molecular viscosity and conductivity is caused by high flow velocities, at which the molecular mechanisms of momentum and heat transfer are indeed not of primary importance as compared to turbulent transfer mechanisms. On the contrary, the turbulence has a significant effect on the processes of mass, momentum, and heat transfer in boundary layers on the walls (in particular, on the possible deposition of droplets) as well as it can play an important part in forming condensation shocks and shock waves under conditions of supercooled steam flow.

Therefore, the objective of the paper is to analyze the effect of turbulence on the process of steady and unsteady spontaneous condensation of supercooled steam flow in the absence and the presence of initial moisture in the inlet section of the nozzle. It should be noted that the effect of turbulence on spontaneously condensing flow can be due to two mechanisms: (i) the turbulent transfer of mass, momentum, and heat, which forms the "hydrodynamic pattern" of the flow, and (ii) the turbulent fluctuations of thermodynamic parameters affecting the rates of nucleation and droplet growth. This paper deals with the effect of the former mechanism alone, because a preliminary analysis reveals that the effect of the latter mechanism turns out to be less significant. In the future paper, we will treat the effect of turbulent fluctuations of temperature on the rates of nucleation and condensation growth of droplets.

2. Background of the model

In this study we consider two-phase high-velocity turbulent flows with small droplets arising during the process of spontaneous steady and unsteady condensation of supercooled steam or entering the nozzle. The response time τ_p of such the droplets is assumed to be far shorter than the

* Corresponding author. Tel.: +7 495 150 82 85; fax: +7 495 159 94 74.
E-mail addresses: avetis@dol.ru (A.R. Avetissian), leonid.zaichik@mtu-net.ru (L.I. Zaichik).

0017-9310/$ - see front matter © 2008 Elsevier Ltd. All rights reserved.
doi:10.1016/j.ijheatmasstransfer.2007.11.056

Nomenclature

a_0	dimensionless acceleration magnitude
C_P	heat capacity
$C_{\varepsilon 1}$, $C_{\varepsilon 2}$, C_μ, C_1	turbulence constants
d	droplet diameter
f_u	droplet response coefficient
H	enthalpy
h	half-width or radius of the nozzle
I	nucleation rate
J	condensation/evaporation rate
k_B	Boltzmann constant
k	turbulence energy
L	nozzle length
L_n	moments of the PDF
M	liquid mass per unit volume
M_{mol}	molecular mass
m	droplet mass
N	number of droplets per unit volume
N_A	Avogadro number
P	pressure
Pr_T	turbulent Prandtl number
R	gas constant
Re_λ	Reynolds number
r	droplet radius
S_k, S_ε	turbulence modulation terms
T	steam temperature
T_L	Lagrangian integral timescale
V_i	droplet velocity
$\langle u_i' t' \rangle$	turbulent heat fluxes
$\langle u_i' u_j' \rangle$	turbulent stresses
W_i	velocity of two-phase medium
X	mass fraction of droplets
x_i	space coordinate
z	turbulence parameter

Greek symbols

ΔH	latent heat of vaporization
ΔT	steam overcooling
δ	delta-function
ε	turbulence dissipation rate
θ	droplet temperature
λ	thermal conductivity
ν	kinematic viscosity
ν_T	turbulent viscosity
Π	turbulence production rate
P_m	probability density function of mass distribution
ρ	density
σ	surface tension
σ_k, σ_ε	turbulence constants
τ	time
τ_k	Kolmogorov time scale
τ_p	droplet response time
τ_T	Taylor time microscale
Φ	droplet volume fraction
χ	turbulence intensity
Ψ_L	Lagrangian autocorrelation function
Ω	droplet response parameter

Subscripts

g	gas
l	liquid
s	saturation
0	nozzle inlet
*	critical nucleus

integral time scale of turbulence T_L. Moreover, the mass fraction of droplets (of the moisture) is supposed to be rather low ($X \equiv M/\rho < 0.1$). In this case, the transport and heat/mass transfer of steam–droplet medium may be governed by the conservation equations of mass, momentum, and energy for a two-phase flow as a whole by neglecting the effects of molecular viscosity and conductivity

$$\frac{\partial \rho}{\partial \tau} + \frac{\partial \rho W_i}{\partial x_i} = 0, \tag{1}$$

$$\frac{\partial \rho W_i}{\partial \tau} + \frac{\partial \rho W_i W_j}{\partial x_j} = -\frac{\partial P}{\partial x_i} - \frac{\partial \rho \langle u_i' u_j' \rangle}{\partial x_j}, \tag{2}$$

$$\frac{\partial \rho H}{\partial \tau} + \frac{\partial \rho W_i H}{\partial x_i} = -\frac{\partial C_P \langle u_i' t' \rangle}{\partial x_i} + \frac{\partial P}{\partial \tau} + W_i \frac{\partial P}{\partial x_i} + \rho \varepsilon. \tag{3}$$

Here $\rho \equiv (1 - \Phi)\rho_g + \Phi\rho_l \approx \rho_g + M$ is the density of the two-phase steam–droplet medium; ρ_g and ρ_l are the densities of the gaseous and liquid phases; $M \equiv \Phi\rho_l$ is the mass of the liquid phase per unit volume; Φ is the volume fraction of the liquid phase; W_i, H, and C_P are the velocity, the enthalpy, and the heat capacity of the two-phase medium, respectively; P is the pressure; and ε denotes the dissipation rate of turbulence energy.

The nucleation rate due to spontaneous condensation is predicted using the classic Volmer–Frenkel–Zel'dovich theory

$$I = \left(\frac{N_A}{M_{mol}}\right)^{3/2} \frac{\rho_g^2}{\rho_l} \left(\frac{2\sigma}{\pi}\right)^{1/2} \exp\left(-\frac{4\pi\sigma r_*^2}{3k_B T}\right), \tag{4}$$

where σ is the surface tension coefficient, and T is the temperature of the steam.

In (4), the critical radius of nucleation is determined by the Kelvin formula

$$r_* = \frac{2\sigma}{\rho_l R T \ln(P/P_s)},$$

where P_s denotes the saturation pressure on a flat surface (at $r=\infty$), which corresponds to the temperature of the steam T.

The rate of heterogeneous phase transitions depends on the droplet size (the Knudsen number). The condensation/evaporation rate of fine droplets at large Knudsen numbers is given by the kinetic Hertz–Knudsen model for the free-molecule regime

$$J = J_K = \frac{4\pi r^2 P}{\sqrt{2\pi RT}}\left(1-\sqrt{\frac{T}{\theta}}\right). \tag{5}$$

In (5), the temperature of droplets is found from the condition of equality of the saturated steam pressure at the curved surface of droplets to the pressure of the surrounding flow. Whence it follows that

$$\theta = T_s - (T_s - T)\frac{r_*}{r},$$

where T_s stands for the saturation temperature on a flat surface (at $r=\infty$), which corresponds to the pressure of the steam P. Note that the condensation/evaporation coefficients, which are usually introduced into the kinetic model (5), are taken to be equal to unity.

The rate of phase transitions for the continuum regime, i.e., for the case of relatively large droplets at low Knudsen numbers, is limited by the removal (during condensation) or the input (during evaporation) of the heat of vaporization. In accordance with this, the rate of phase transitions is controlled by the thermal resistance between the droplet surface and the surrounding medium

$$J = J_T = \frac{4\pi r\lambda(\theta - T)}{\Delta H}, \tag{6}$$

where λ is the thermal conductivity of the gaseous phase, and ΔH is the latent heat of vaporization.

In order to determine the rate of condensation/evaporation in the entire range of varying Knudsen numbers, the interpolation equation is used that combines (5) and (6)

$$J = \frac{J_K J_T}{J_K + J_T}. \tag{7}$$

The evolution of droplet size spectrum in time and space due to homogeneous and heterogeneous phase transitions is governed by a kinetic equation for the probability density function (PDF) of mass distribution

$$\frac{\partial P_m}{\partial \tau} + \frac{\partial V_i P_m}{\partial x_i} + \frac{\partial J P_m}{\partial m} = I\delta(m - m_*), \tag{8}$$

where $m \equiv 4\pi\rho_l r^3/3$ is the droplet mass. In (8), the two first terms on the left-hand side describe, respectively, the change in time and the convection in space, whereas the last term on the left side and the first term on the right side quantify the evolution of the droplet mass distribution due to heterogeneous (condensation or evaporation) and homogeneous (nucleation) phase transitions. The velocity of the droplet phase V_i is taken to be equal to the velocity of the two-phase medium W_i.

To solve (8) we invoke the moment method that is based on employing equations for the moments of the PDF. These are derived as a result of integrating (8) multiplied by m^k over the droplet mass spectrum

$$\begin{aligned} &\frac{\partial L_n}{\partial \tau} + \frac{\partial V_i L_n}{\partial x_i} = I m_*^n + n\int_0^\infty m^{n-1} J P_m(m)\,\mathrm{d}m, \\ &L_n = \int_0^\infty m^n \mathrm{P}_m\,\mathrm{d}m. \end{aligned} \tag{9}$$

In the free-molecule regime of condensation/evaporation (at $r \gg r_*$), when the rate of phase transitions according to (5) is determined by the relationship $J = am^{2/3}$ with $a = \text{const}$, it is expedient that the characteristic moments describing the size (mass) distribution of droplets should be provided by L_n at $n = 0,\ 1/3,\ 2/3,\ 1$ [7]. In this case, the set of Eq. (9) becomes closed and thereby all of the PDF moments of interest may be found. In the general case when the rate of phase transitions is determined by (7) and hence can be represented as $J = a(m)m^{2/3}$, the set of Eq. (9) amounts approximately to

$$\begin{aligned} &\frac{\partial L_n}{\partial \tau} + \frac{\partial V_i L_n}{\partial x_i} = I m_*^n + n a(\bar{m}_n) L_{n-1/3}, \\ &\bar{m}_n = \left(\frac{L_n}{L_{n-1/3}}\right)^3, \quad n = 0, 1/3, 2/3, 1. \end{aligned} \tag{10}$$

It should be noted that $L_0 \equiv N$ and $L_1 \equiv M$ are, respectively, the number and mass of droplets per unit volume.

When considering the initial moisture supplied to the nozzle inlet, we solve two-equation sets of (10) for two droplet ensembles. The first equation set describes the ensemble of the droplets which are formed due to the spontaneous condensation of supercooled steam, and the second one quantifies the evolution of the droplets entering the nozzle.

3. Turbulence model

Turbulent flow characteristics are simulated on the basis of a two-equation turbulence model incorporating the equations of kinetic turbulence energy and its dissipation, that is, the k–ε turbulence model. In the frame of the k–ε turbulence model, the Reynolds stresses and the turbulent heat fluxes are defined by Boussinesq–Fourier's gradient relationships with an isotropic turbulent viscosity

$$\begin{aligned} &\langle u_i' u_j' \rangle = \frac{2}{3}k\delta_{ij} - \nu_T\left(\frac{\partial W_i}{\partial x_j} + \frac{\partial W_j}{\partial x_i} - \frac{2}{3}\frac{\partial W_k}{\partial x_k}\delta_{ij}\right), \\ &\langle u_i' t' \rangle = -\frac{\nu_T}{\mathrm{Pr}_T}\frac{\partial T}{\partial x_i}. \end{aligned} \tag{11}$$

For two-phase flows with relatively small mass fractions and sizes of droplets, the difference between the velocity of the two-phase flow as a whole and that of the gaseous phase may be neglected. Consequently, (11) contains the velocity of the two-phase flow rather than that of the gaseous phase.

The equations of turbulence energy and its dissipation rate are represented in the form that is appropriate at high-Reynolds numbers

$$\frac{\partial \rho k}{\partial \tau}+\frac{\partial \rho W_i k}{\partial x_i}=\frac{\partial}{\partial x_i}\left(\frac{\rho \nu_{\mathrm{T}}}{\sigma_k}\frac{\partial k}{\partial x_i}\right)+\rho\Pi-\rho\varepsilon+S_k, \tag{12}$$

$$\frac{\partial \rho \varepsilon}{\partial \tau}+\frac{\partial \rho W_i \varepsilon}{\partial x_i}=\frac{\partial}{\partial x_i}\left(\frac{\rho \nu_{\mathrm{T}}}{\sigma_\varepsilon}\frac{\partial \varepsilon}{\partial x_i}\right)+\rho\frac{\varepsilon}{k}(C_{\varepsilon 1}\Pi-C_{\varepsilon 2}\varepsilon)+S_\varepsilon, \tag{13}$$

where $\Pi \equiv -\langle u_i' u_j' \rangle \partial W_i/\partial x_j$ denotes the production rate of turbulence energy, and S_k and S_ε designate the source terms due to droplets.

In the frame of the standard k–ε turbulence model, the turbulent viscosity coefficient is given by

$$\nu_{\mathrm{T}}=C_\mu\frac{k^2}{\varepsilon}. \tag{14}$$

The values of constants in (11)–(14) are usually taken to be as follows: $C_\mu=0.09$, $\sigma_k=1.0$, $\sigma_\varepsilon=1.3$, $C_{\varepsilon 1}=1.44$, $C_{\varepsilon 2}=1.92$, $Pr_{\mathrm{T}}=0.9$. The standard turbulence k–ε model (the STM), which involves Eqs. (12) and (13) at $S_k=S_\varepsilon=0$ along with (11) and (14), is widely used to calculate flows of various types. However, in spite of great utility owing to its simplicity, the STM suffers from well-known drawbacks. For example, the STM is unable to properly simulate turbulent flows with large velocity gradients, strong contraction or expansion, surface curvature, and so forth. Strictly spiking, this model can be correctly employed only for simulating quasi-equilibrium turbulent flows when the turbulence generation and dissipation rates are approximately equal ($\Pi\approx\varepsilon$). The foregoing reasons make the STM incapable of predicting spontaneously condensing streams in transonic nozzles and blade channels. Therefore, the standard k–ε model is modified in two aspects. Firstly, the modulation of turbulence due to droplets is taken into consideration. Secondly, instead of standard expression (14) for the eddy viscosity coefficient, this coefficient is assumed to be a function of the turbulence production-to-dissipation ratio.

The source term accounting for the modulation of the turbulence energy due to additional dissipation by droplets is represented in the form

$$S_k=\frac{2M}{\tau_p}(1-f_u)k,$$

$$f_u=\frac{1}{\tau_p}\int_0^\infty \Psi_{\mathrm{L}}(\tau)\exp\left(-\frac{\tau}{\tau_p}\right)\mathrm{d}\tau, \tag{15}$$

where f_u is the coefficient of droplet response to the fluid velocity fluctuations, and $\Psi_{\mathrm{L}}(\tau)$ is the Lagrangian velocity autocorrelation function of a fluid element moving along a droplet trajectory. To determine f_u, a two-scale bi-exponential approximation of the autocorrelation function by Sawford [8] is used. This approximation leads to the following formula for the response coefficient [9]:

$$f_u=\frac{2\Omega+z^2}{2\Omega+2\Omega^2+z^2},\quad \Omega=\frac{\tau_p}{T_{\mathrm{L}}},\quad z=\frac{\tau_{\mathrm{T}}}{T_{\mathrm{L}}},$$

where the turbulence parameter z measures the ratio of the Lagrangian integral timescale to the Taylor differential timescale of velocity fluctuations.

The Lagrangian integral timescale is determined by the relationship

$$T_{\mathrm{L}}=C_\mu^{1/2}\frac{k}{\varepsilon}.$$

The Taylor time microscale is given by

$$\tau_{\mathrm{T}}=\left(\frac{2Re_\lambda}{15^{1/2}a_0}\right)^{1/2}\tau_{\mathrm{k}},\quad \tau_{\mathrm{k}}=\left(\frac{\nu}{\varepsilon}\right)^{1/2},$$

$$Re_\lambda=\left(\frac{20k^2}{3\varepsilon\nu}\right)^{1/2},\quad a_0=7,$$

where the value of a_0 is taken in accordance with experimental date at large Reynolds numbers [10].

The source term in Eq. (13) is assumed to be proportional to the corresponding one that appears in Eq. (12)

$$S_\varepsilon=C_{\varepsilon 2}\frac{\varepsilon}{k}S_k. \tag{16}$$

The turbulent viscosity coefficient is derived by means of an expansion procedure for resolving implicit algebraic equations for Reynolds stress tensor in terms of mean velocity gradients [11,12]. The first term of this expansion gives

$$\nu_{\mathrm{T}}=\frac{C_\mu}{1+(\Pi/\varepsilon-1)/C_1}\frac{k^2}{\varepsilon}. \tag{17}$$

As is seen, the turbulent viscosity coefficient given by (17) is dependent on the turbulence production-to-dissipation ratio, and it contains an additional constant C_1 respect to the STM. This constant is the familiar one in the Rotta return-to-isotropy approximation of the pressure–strain correlation. When $C_1\to\infty$, (17) reduces to the STM coefficient (14). The turbulence model incorporating (11)–(13) along with (15)–(17) is further referred to as the modified turbulence k–ε model (the MTM). The minimum permissible for C_1 equals to unity [13]. When $C_1=1$, (17) becomes particularly simple, namely, $\nu_{\mathrm{T}}=C_\mu k^2/\Pi$. However, as was demonstrated for the first time by Sarkar and Speziale [14], the Rotta constant plays an important part in the stability of turbulent flow and, with a view to ensuring stability, it should assume a value which exceeds unity. To provide good agreement with experiments and direct numerical computations, C_1 must not too far remove from unity (e.g. [15]). Therefore, this constant is further taken as 1.1.

It is worth to emphasize that the implantation of (17) instead of (14) into a computational code does not require any changing numerical procedure employed for the standard k–ε model. Therefore, the standard wall function as the boundary conditions can be used [16].

4. Calculation results and discussion

Computations have been performed for transonic wet-steam flows under the conditions corresponding to the experimental investigations for flat nozzles by Barschdorff [17] and Skillings et al. [18] as well as for a round nozzle by Deich and Philippov [19] in both the absence and the presence of initial moisture supplied to the nozzle inlet. The motion and heat/mass transfer of the two-phase medium is governed by the set of Eqs. (1), (2), (3), (10), (12) and (13). Calculations were performed in a two-dimensional formulation. Particular attention has been paid to conditions producing either steady or unsteady flow because of condensation phenomena and turbulence effects. With this object in mind, the total pressure P_0, the temperature T_0, and the moisture X_0 in the nozzle inlet were varied. Moreover, the computations were conducted at various values of the inlet turbulence intensity $\chi_0 = (k^{1/2}/W)_0$. The inlet turbulence dissipation rate was given by the relationship $\varepsilon_0 = k_0^{3/2}/h_0$ where h_0 denotes the inlet half-width or the radius of the nozzle.

First consider simulation results with no initial moisture entering the nozzle, when the dry steam is supplied to the nozzle inlet and hence the droplets are forming due to only spontaneous condensation. When the dry steam with an inlet state near the saturation line is expanded through a Laval nozzle, its supercooling may attain a level of 30–40 K in the supersonic part of the flow. Such a supercooling causes the spontaneous condensation inducing an increase in pressure. This pressure rise can be quite steep, that is why it was named the condensation shock.

Figs. 1–3 present the predictions conforming, respectively, to experiments by Barschdorff [17] with $P_0 = 78{,}100$ Pa and $T_0 = 376$ K as well as by Skillings et al. [18] with $P_0 = 367{,}000$ Pa and $T_0 = 353$ K for the conditions when the steady condensation shock exists. From Fig. 1, where the Mach number contours are given, one can observed the overall pattern of the flow including

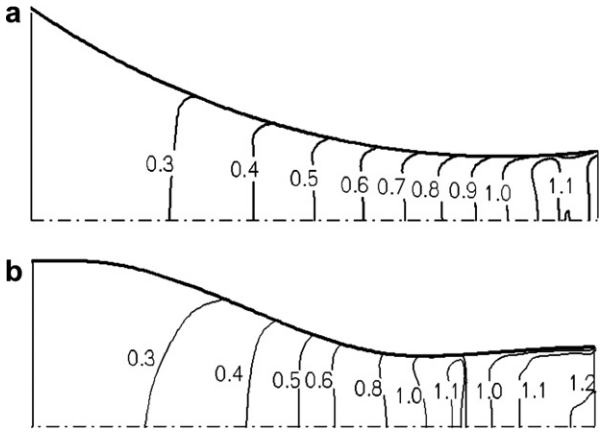

Fig. 1. Mach number counters. (a) Barschdorff [17], (b) Skillings et al. [18].

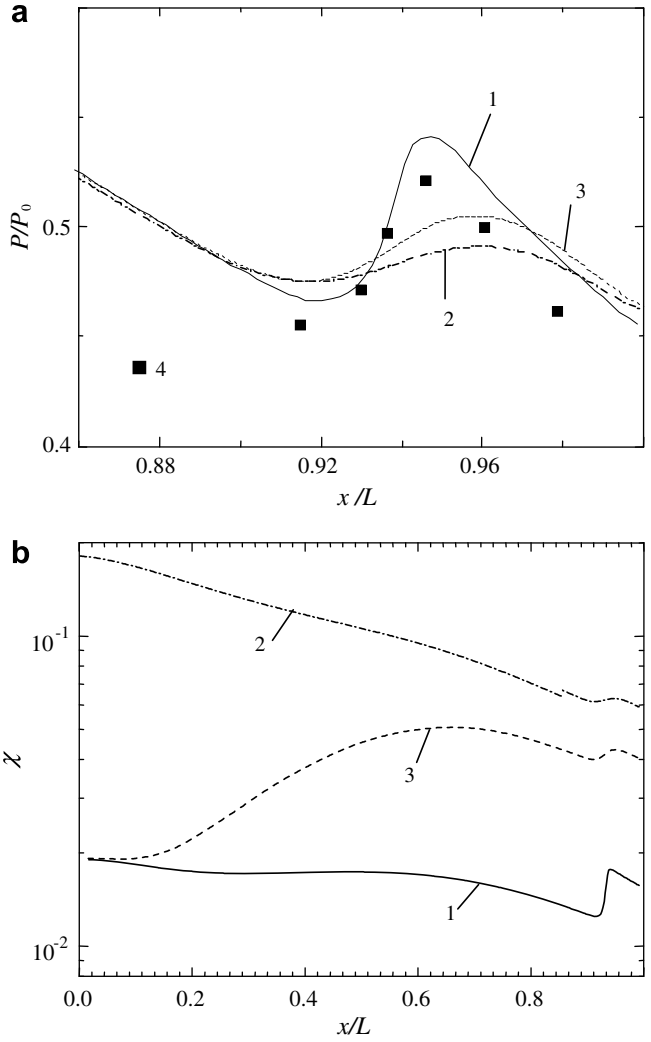

Fig. 2. Variations in pressure (a) and turbulence intensity (b) along the nozzle axis. (1) MTM for $\chi_0 = 0.02$, (2) MTM for $\chi_0 = 0.2$, (3) STM for $\chi_0 = 0.02$, (4) experiments by Barschdorff [17].

the shapes of the nozzles being considered. Figs. 2 and 3a show the axial variation in pressure normalized by the total inlet pressure as a function of the distance from the nozzle inlet x scaled by the nozzle length L. The corresponding axial distributions of the turbulence energy scaled by the mean axis velocity are displayed in Figs. 2 and 3b. It is seen that the distributions of pressure along the nozzle predicted by means of the MTM for low-level inlet turbulence ($\chi_0 = 0.02$) are found to be in accordance with experimental data, including the shape and the position of the condensation chock. However, they differ drastically from those derived with the help of both the MTM for high-level inlet turbulence ($\chi_0 = 0.2$) and the STM for low-level inlet turbulence. Because of great values of the eddy viscosity in the near-axis region of the nozzle at high-level inlet turbulence, the condensation chock spreads out, and the axial distributions of pressure and other flow parameters become quiet. As is clear from Figs. 2 and 3b (curves 3), the STM predicts too high a level of turbulence even with a low inlet

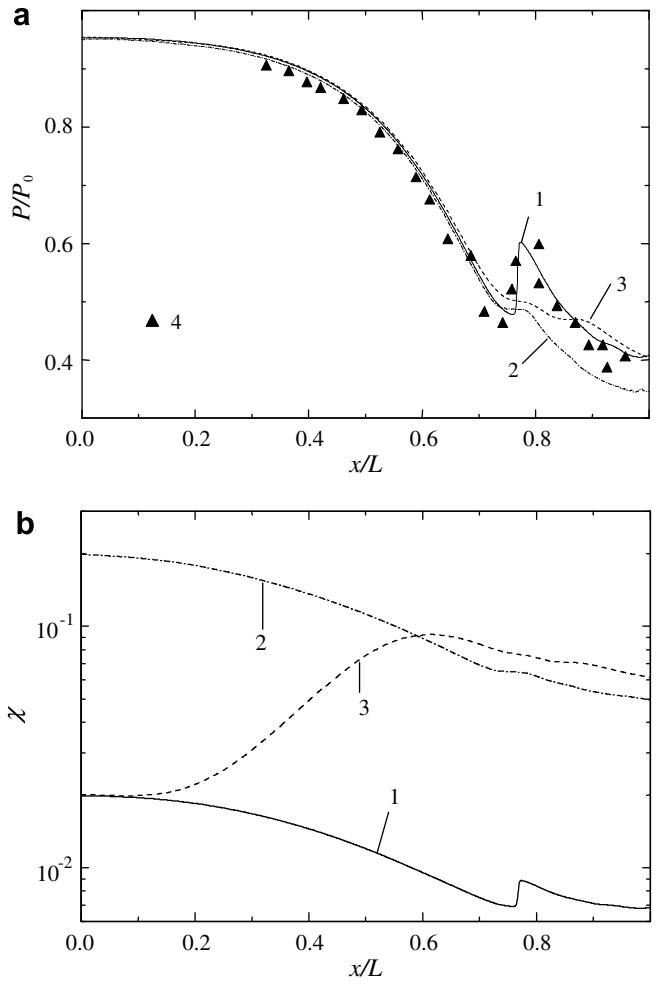

Fig. 3. Variations in pressure (a) and turbulence intensity (b) along the nozzle axis. (1) MTM for $\chi_0 = 0.02$, (2) MTM for $\chi_0 = 0.2$, (3) STM for $\chi_0 = 0.02$, (4) experiments by Skillings et al. [18].

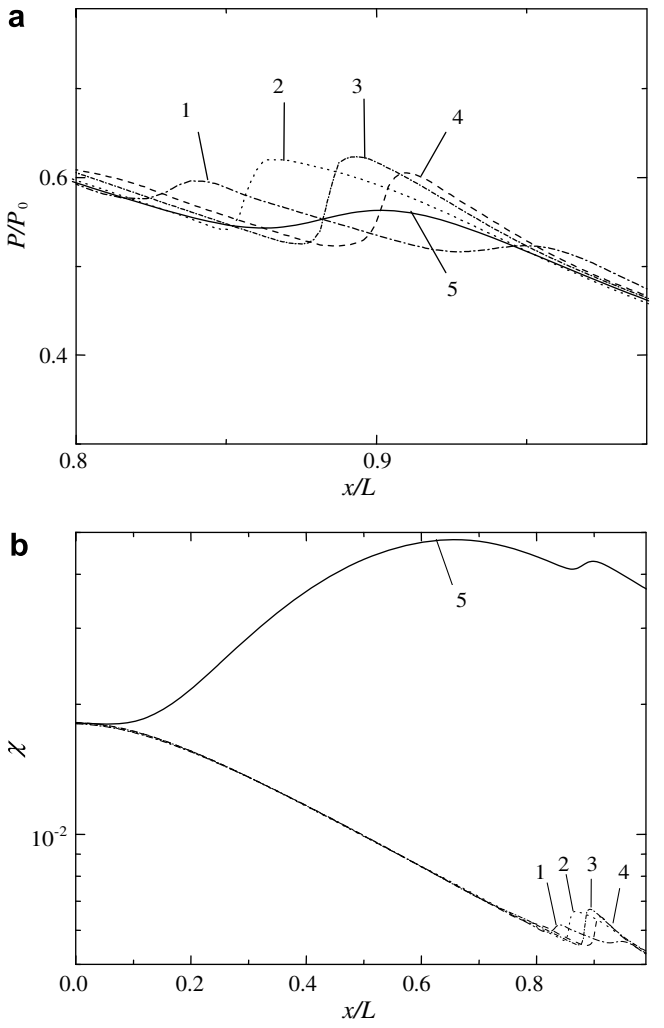

Fig. 4. Distributions of pressure (a) and turbulence intensity (b) along the nozzle by Barschdorff [17] at different time moments. (1)–(4) MTM, (5) STM.

value, this also leading to the disappearance of the condensation chock.

When reducing the inlet overheat, the steady condensation shock moves upstream into the throat of the nozzle. This results eventually in the crisis of steady flow whereby an unsteady self-oscillating flow is achieved. The self-induced oscillations emerge due to the feedback mechanism that is realized by shock waves: while moving counter to the flow, these waves lower the supercooling of steam and, thereby, eliminate the cause of their formation (i.e., spontaneous condensation). Thereafter a supersonic expansion with accompanying condensation is re-established and the process repeats, giving the self-induced oscillations of every flow property.

Figs. 4 and 5 present the predictions, which correspond, respectively, to experiments by Barschdorff [17] with $P_0 = 93{,}400$ Pa and $T_0 = 376$ K as well as by Skillings et al. [18] with $P_0 = 351{,}000$ Pa and $T_0 = 348$ K for the conditions when the self-oscillating shock waves take place. In these figures, curves 1–4 display, at different moments of time, the pressure and turbulence intensity distributions predicted by means of the MTM for low-level inlet turbulence ($\chi_0 = 0.02$). The predicted frequencies of 840 and 410 Hz compare well with the measured ones of 810 and 380 Hz obtained, respectively, in experiments by Barschdorff [17] and by Skillings et al. [18]. From Figs. 4 and 5, it is also clear that the STM results in dissipating the condensation shock waves (curves 5). Thus, the STM can lead to predicting a fallacious mode and a wrong structure of the flow.

Figs. 6 and 7 demonstrate the influence of the inlet turbulence intensity on pressure oscillations at the nozzle axis near the exit section. All the curves shown in Figs. 6 and 7 were predicted using the MTM. The main effect seen consists in dissipating the condensation shock waves for high-level inlet turbulence.

In what follows let us examine the impact of inlet moisture on condensation phenomena. In qualitative sense, this impact resembles the effect of high-level turbulence, namely, the initial moisture can result in a complete

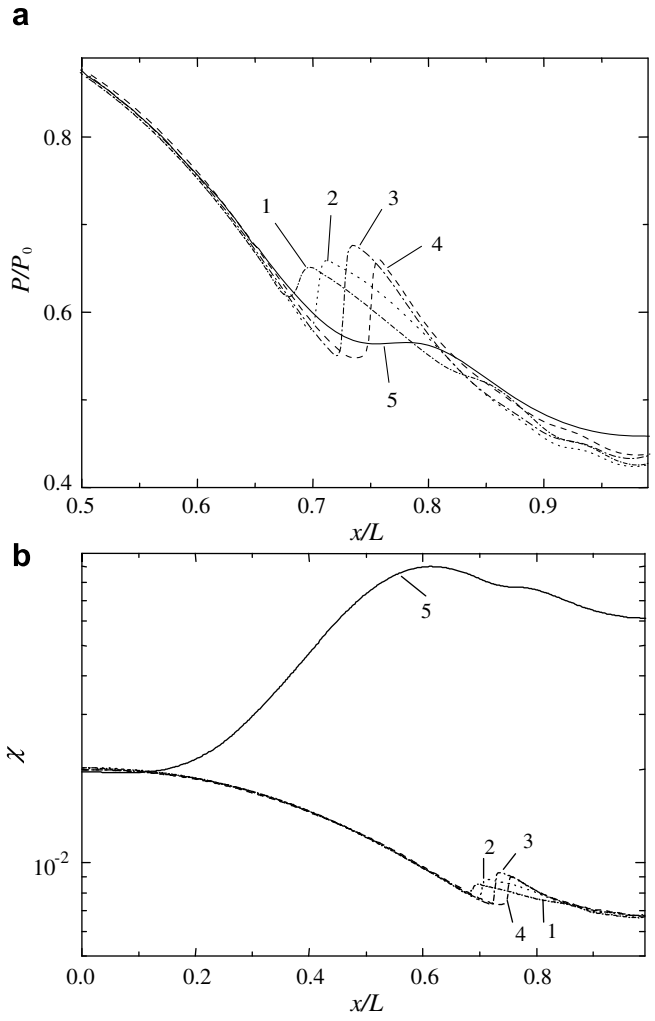

Fig. 5. Distributions of pressure (a) and turbulence intensity (b) along the nozzle by Skillings et al. [18] at different time moments. (1)–(4) MTM, (5) STM.

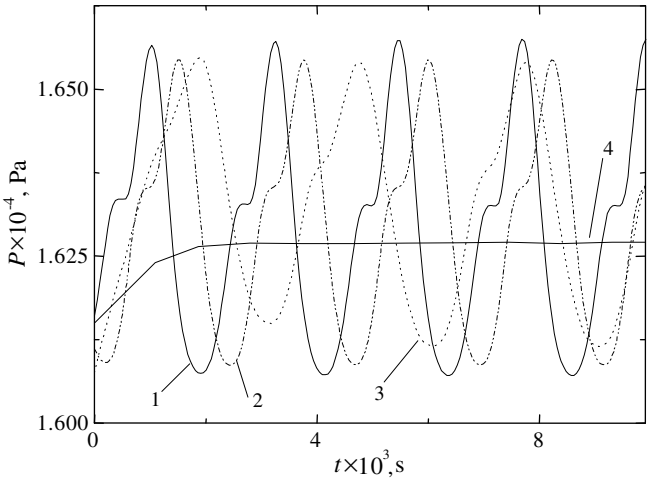

Fig. 7. Pressure oscillations in the nozzle by Skillings et al. [18]. (1) $\chi_0 = 0.02$, (2) 0.06, (3) 0.10, (4) 0.15.

disappearance of the condensation chock. This is caused by a decrease in steam overcooling due to condensation on the droplets supplied to the nozzle inlet. The influence of inlet wetness X_0 reduces with increasing initial mean-volume droplet diameter d_0, because the effect is proportional to the condensation surface. Fig. 8 shows predicted and measured variations in pressure along a round nozzle, when the total pressure in the nozzle inlet was fixed and equal to 3.16×10^4 Pa, whereas the total inlet temperature and moisture were changed [19]. Therefore, Fig. 8 demonstrates the impact of inlet steam overheating and moisture on the process of spontaneous condensation. It is seen that, in accordance with the experimental date, the pressure rise induced by spontaneous condensation decreases with increasing both inlet steam overheating and inlet moisture. Moreover, like the effect of high-level inlet turbulence, the inlet moisture can lead not only to the disappearance of a stationery condensation shock

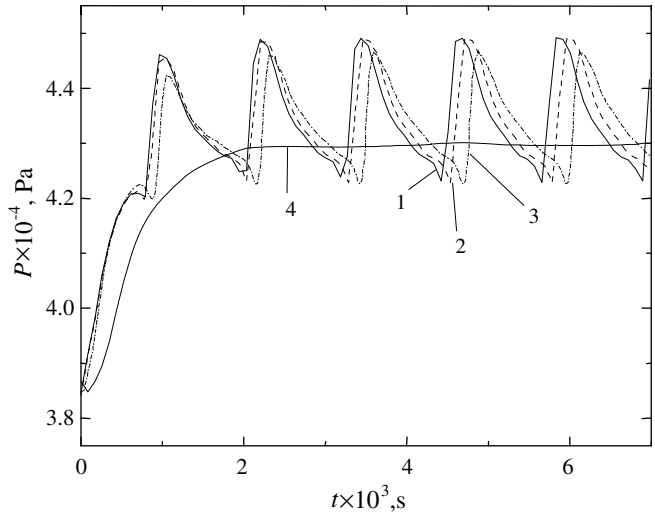

Fig. 6. Pressure oscillations in the nozzle by Barschdorff [17]. (1) $\chi_0 = 0.02$, (2) 0.04, (3) 0.06, (4) 0.10.

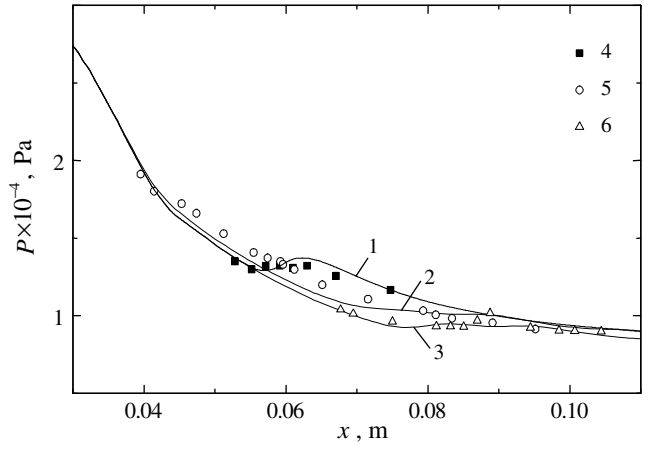

Fig. 8. Predicted (1–3) and measured (4–6) variations in pressure along the nozzle by Deich and Philippov [19]. (1) and (4) – $T_0 = 352$ K, $X_0 = 0$; (2) and (5) – $T_0 = 352$ K, $X_0 = 0.004$; (3) and (6) – $T_0 = 370$ K, $X_0 = 0$.

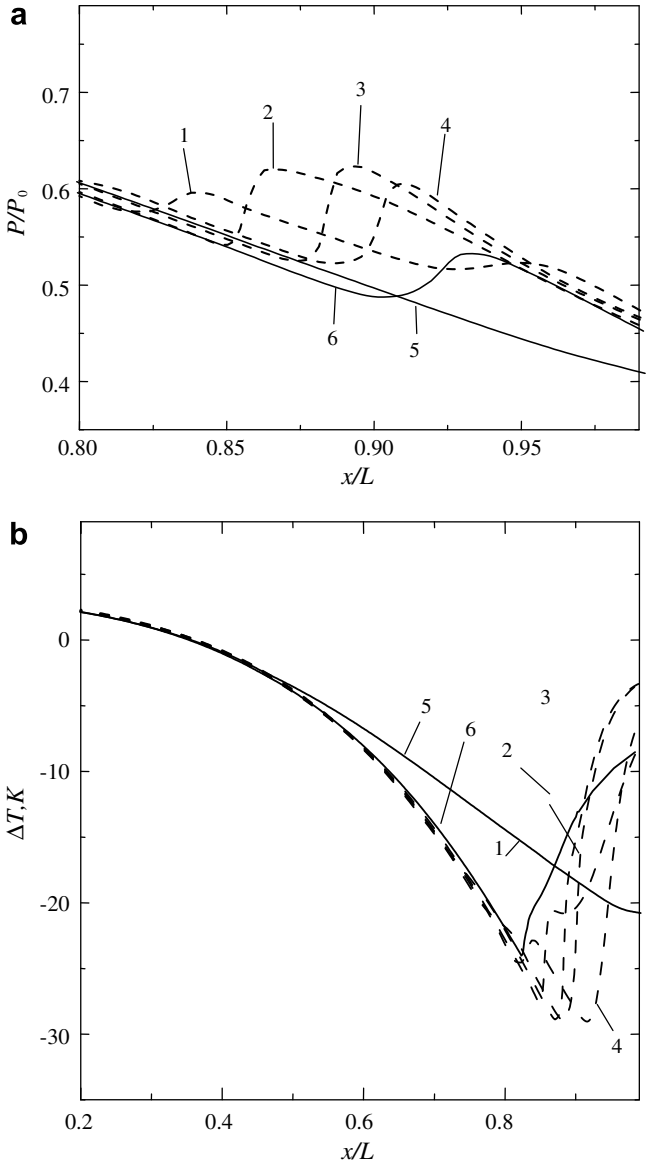

Fig. 9. The effect of inlet moisture on the variations in pressure (a) and steam overcooling (b) along the nozzle by Barschdorff [17]. (1)–(4) $X_0 = 0$; (5) $X_0 = 0.001$, $d_0 = 0.01$ μm; (6) $X_0 = 0.001$, $d_0 = 0.4$ μm.

but can result in dissipating the condensation shock waves as well. This is evident from Fig. 9 where the distributions of pressure and steam overcooling ($\Delta T \equiv T - T_s$) along the nozzle by Barschdorff [17] for $P_0 = 78{,}100$ Pa and $T_0 = 376$ K are shown.

5. Summary

The main findings obtained from the simulations performed can be given as follows:

(i) The standard k–ε turbulence model can be invalid for predicting two-phase flows in transonic nozzles. This model may bring about incorrect results, namely, the disappearance of both a steady condensation shock and unsteady shock waves even in the case of a low-level of inlet turbulence.

(ii) The modified k–ε turbulence model compares well with experimental date and properly reproduces the crucial trends of steady and unsteady spontaneously condensing flows in Laval nozzles.

(iii) The effect of high-level inlet turbulence causes the steady chock and the shock waves of spontaneous condensation to disappear.

(iv) The influence of inlet moisture on spontaneously condensing flow resembles the effect of turbulence. In particular, the steady shock and the shock waves can be completely disappeared as a consequence of a decrease in steam overcooling due to condensation of the steam on the droplets entering the nozzle.

Acknowledgement

This work was supported by the Russian Foundation for Basic Research (Grant Numbers 06-08-01488 and 07-08-00672).

References

[1] S.A. Skillings, R. Jackson, A robust time-marching solver for one-dimensional nucleating steam flows, Int. J. Heat Fluid Flow 8 (1987) 139–144.
[2] C.F. Delale, G.H. Schnerr, J. Zierep, Asymptotic solution of transonic nozzle flows with homogeneous condensation. I. Subcritical flows, Phys. Fluids A 5 (1993) 2969–2981.
[3] A.J. White, J.B. Young, Time-marching method for the prediction of two-dimensional, unsteady flows of condensing steam, J. Prop. Power 9 (1993) 579–587.
[4] A.R. Avetissian, V.M. Alipchenkov, L.I. Zaichik, Simulation of a flow of spontaneously condensing moist steam in Laval nozzles, High Temp. 40 (2002) 872–880.
[5] F. Bakhtar, A.J. White, H. Mashmoushy, Theoretical treatments of two-dimensional two-phase flows of steam and comparison with cascade measurements, J. Mech. Eng. Sci. 219 (2005) 1335–1355.
[6] G.H. Schnerr, Unsteadiness in condensing flow: dynamics of internal flows with phase transition and application to turbomachinery, J. Mech. Eng. Sci. 219 (2005) 1369–1410.
[7] P.G. Hill, Condensation of water vapour during supersonic expansion in nozzles, J. Fluid Mech. 25 (1966) 593–620.
[8] B.L. Sawford, Reynolds number effects in Lagrangian stochastic models of turbulent dispersion, Phys. Fluids A 3 (1991) 1577–1586.
[9] L.I. Zaichik, O. Simonin, V.M. Alipchenkov, Two statistical models for predicting collision rates of inertial particles in homogeneous isotropic turbulence, Phys. Fluids 15 (2003) 2995–3005.
[10] G.A. Voth, K. Satyanarayan, E. Bodenschatz, Lagrangian acceleration measurements at large Reynolds numbers, Phys. Fluids 10 (1998) 2268–2280.
[11] C.G. Speziale, On nonlinear k–l and k–ε models of turbulence, J. Fluid Mech. 178 (1987) 459–475.
[12] T.B. Gatski, C.G. Speziale, On explicit algebraic stress models for complex turbulent flows, J. Fluid Mech. 254 (1993) 59–78.

[13] J.L. Lumley, The second-order models of turbulent flows, in: Prediction Methods for Turbulent Flows, Hemisphere, New York, 1980.
[14] S. Sarkar, C.G. Speziale, A simple nonlinear model for the return to isotropy in turbulence, Phys. Fluids A 2 (1990) 84–93.
[15] R. Abid, C.G. Speziale, Predicting equilibrium states with Reynolds stress closures in channel flow and homogeneous shear flow, Phys. Fluids A 5 (1993) 1776–1782.
[16] B.E. Launder, D.B. Spalding, The numerical computation of turbulent flows, Comput. Methods Appl. Mech. Eng. 3 (1974) 269–289.
[17] D. Barschdorff, Droplet formation, influence of shock waves and in stationary flow patterns by condensation phenomena at supersonic speeds, in: Proceedings of the International Conference of Rain Erosion and Associated Phenomena, Farnborough, 1970, pp. 691–705.
[18] S.A. Skillings, P.T. Walters, M.J. Moore, A study of supercritical heat addition as potential loss mechanism in condensing steam turbines, in: Int. Mech. Eng. Conf., vol. C259/87, 1987, pp. 125–134.
[19] M.E. Deich, G.A. Philippov, Gasodynamics of Two-Phase Media, Energoatomizdat, Moscow, 1981.